Proceeding of the 18th INFATS & 27th SAE-C/STC, 2024, pp1-10
2024.308

Driver Steering Torque Estimation and Active FuzzyAssistance Control of Vehicle Path Tracking Systems

Wenfeng LI[1], Zheng LIAN[1], Jing ZHAO[1*], Zhengchao XIE[2], Pak Kin Wong[3,4]

[1]*Department of Mechanical Engineering and Automation, Northeastern University, Shenyang 110004, China*

[2]*Department of Mechanical Engineering, South China University of Technology, Guangzhou 510641, China*

[3]*Department of Electromechanical Engineering, University of Macau, Taipa 999078, Macau*

[4]*Zhuhai UM Science and Technology Research Institute, Zhuhai 519085, China*

Email: zhaoj@mail.neu.edu.cn

Abstract: In this paper, an active fuzzy assistance method is proposed for vehicle path tracking system based on driver steering torque estimation. First of all, in order to describe the driver's steering behavior, vehicle kinematics and lateral dynamics, a driver-vehicle-road (DVR) system model is established. The parameter uncertainties are approximated by an interval type-2 (IT-2) fuzzy model. Secondly, to acquire the information of driver steering torque, an adaptive observer is introduced to estimate the driver steering torque effectively. At the same time, the unmeasured system states are also estimated by the observer. Then, an adaptive steering controller is proposed to reduce the driver's burden and enhance the performance of vehicle path tracking. Finally, the effectiveness of the proposed method is verified by simulation.

Keywords: vehicle dynamics control, path tracking control, assistance control, torque estimation, fuzzy model.

1 Introduction

In order to ensure the driving safety, drivers must maintain control of the vehicle before the advent of the era of fully automatic driving. However, under the influence of various factors, drivers may still make operational errors [1, 2]. To reduce the driver's driving burden and reduce the occurrence of traffic accidents, various advanced driver assistance systems have been developed [3]. Therefore, the driver assistance system has been paid more and more attention by the academia and the industry.

The path tracking is one of the basic functions of autonomous vehicles [4]. In such as a scenario, the driver assistance control objective is to assist the driver to keep the path tracking error as close to zero as possible by adjusting the heading and lateral position of the vehicle [5, 6]. In order to design the driver assistance controller, it is necessary to establish an accurate DVR system model. Li et al. [7] employed a Takagi-Sugeno (T-S) fuzzy model to characterize the uncertain dynamics of the DVR system by considering both uncertainties in parameters and sampled measurements. The T-S fuzzy model can describe the nonlinearity and uncertainty of the system. And a T-S fuzzy model was constructed for the vehicle path tracking system with communication delay in [8]. Nguyen et al. [9] studied lateral shared control between human drivers and intelligent vehicle lane keeping and obstacle avoidance. The T-S fuzzy control method was proposed for the change of driver activity parameters and vehicle speed with time. However, due to the limitation of sensor performance, it is difficult to measure vehicle longitudinal speed accurately. The inaccurate longitudinal velocity may cause some uncertainties in the membership function of the above T-S fuzzy vehicle model. The IT-2 fuzzy model can effectively deal with the uncertainty of membership functions and is investigated in this work.

The driver's steering torque is widely used to evaluate the driver's attention. To identify the human steering intervention torque, the authors in [10] proposed a model-based estimation strategy for the artificial steering intervention torque of autonomous vehicles. In order to improve the electric power assisted steering system performance and reduce system complexity, the authors in [11] proposed a sliding mode observer to estimate the driver torque and road reaction of electric power steering systems with consideration of unknown inputs. In [12], the authors designed an unknown input observer using a decoupling-based technique to estimate the drive torque and sideslip angle. The above results can accurately estimate the steering torque of the driver and play a great role in explaining the driver's attention. Based on the adaptive torque estimation method, the observer can provide real-time dynamic information of the driver's torque by designing the adaptive updating law of the driver's torque [13]. On this basis, this paper studies an estimation method of driver's steering torque, which is of great significance to determine the active input required by the auxiliary driver. Based on this, this paper proposes an active fuzzy assistance control method based on driver's steering torque observer, which plays an important role in require driver's steering torque and improving vehicle path tracking performance.

The rest of this paper is organized as follows. In Section 2, establish the driver-vehicle-road interval type-2 fuzzy model. Section 3 gives the design results of the observer and controller. Section 4 introduces the simulation results of the designed control method, followed by some concluding remarks in Section 5.

Table 1. Nomenclature

Notation	Definition	Unit
m	Vehicle mass	kg
v_y	Vehicle lateral velocity	m/s
v_x	Vehicle longitudinal velocity	m/s
ψ_v	vehicle heading angle	rad
I_z	Yaw moment inertia	kg·m^2
y_e	Lateral deviation error at l_d	m
ψ_e	Heading error at current position	rad
l_d	look-ahead distance	m
C_a	Cornering stiffness of front wheel	N/rad
C_b	Cornering stiffness of rear wheel	N/rad
δ_d	front wheel steering angle	rad

2 Problem formulation

2.1 Driver-vehicle-road System model

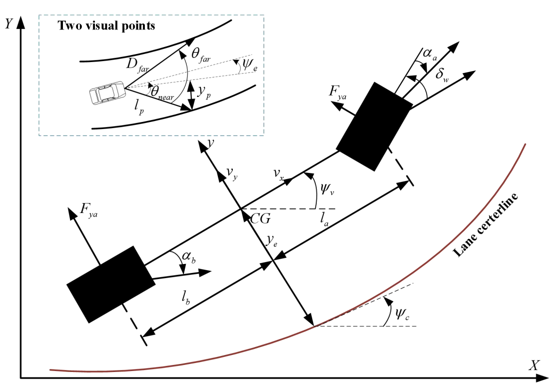

Figure 1. Vehicle lateral kinematics and dynamics model

The single-track model shown in Fig.1 can explain the lateral behavior of the vehicle. It is assumed that both the driver steering angle and sideslip angle are small, and the aerodynamics and vehicle longitudinal dynamics are ignored. The lateral dynamics and kinematics of the vehicle can be expressed as:

$$\begin{cases} m(\dot{v}_y + v_x\dot{\psi}) = C_f(\delta_d - \dfrac{l_f\dot{\psi} - v_y}{v_x}) + C_r(\dfrac{l_r\dot{\psi} - v_y}{v_x}) \\ I_z\ddot{\psi} = l_f C_f(\delta_d - \dfrac{l_f\dot{\psi} - v_y}{v_x}) - l_r C_r(\dfrac{l_r\dot{\psi} - v_y}{v_x}) \end{cases} \tag{1}$$

$$\begin{cases} \dot{\psi}_e = \dot{\psi}_v - v_x\rho(\sigma) \\ \dot{y}_e = v_y + v_x\psi_e + l_d\dot{\psi} \end{cases} \tag{2}$$

The steering system is described as follows:

$$I_s\ddot{\delta}_w + B_s\dot{\delta}_d = \frac{T_d(t) + T_a(t)}{R_s} - \frac{C_a\eta_t}{R_s^2}(\delta_w - \frac{v_y}{v_x} - \frac{l_a\dot{\psi}_v}{v_x}) \tag{3}$$

where I_s is the moment of inertia, B_s is the damping coefficient of the steering system, and R_s is the steering transmission ratio.

The driver torque is described as:

$$T_d(t) = G_c + G_a = k_{s1}\theta_{near} + k_{s2}\theta_{far} \tag{4}$$

where G_c and G_a as the compensatory and anticipatory components of the driver's behavior, respectively. $k_{s1} = -300$, $k_{s2} = -2$ are the driver's proportional actions in accordance with θ_{near} and θ_{far}, separately. To replicate the steering actions of drivers, a two-point preview model is employed, and the compensation behavior and expected behavior are described by near point and far point respectively. Near and far point is defined as:

$$\begin{cases} \theta_{near} = \psi_e + \dfrac{y_p}{l_p} \\ \theta_{far} = \theta_1 v_y + \theta_2\dot{\psi}_v + \theta_3\delta_d \end{cases} \tag{5}$$

where $\theta_1 = \tau_a^2 a_{21}, \theta_2 = \tau_a + \tau_a^2 a_{22}, \theta_3 = \tau_a^2 a_{25}$ and $\tau_a = 0.5$, representing the anticipatory time.

In summary, the human-vehicle road model can be derived as follows:

$$\dot{x}_p(t) = A_p x_p(t) + B_{p1}\omega_s(t) + B_{p2}(T_d(t) + T_a(t)) \tag{6}$$

where the system state vector and matrices are:

$$A_p = \begin{bmatrix} a_{11} & a_{12} & 0 & 0 & a_{15} & 0 \\ a_{22} & a_{23} & 0 & 0 & a_{25} & 0 \\ 1 & l_d & 0 & v_x & 0 & 0 \\ 0 & 1 & 0 & 0 & 0 & 0 \\ 0 & 0 & 0 & 0 & 0 & -1 \\ a_{61} & a_{62} & 0 & 0 & a_{65} & a_{66} \end{bmatrix}, B_{p1} = \begin{bmatrix} 0 \\ 0 \\ 0 \\ -v_x \\ 0 \\ 0 \end{bmatrix}, B_{p2} = \begin{bmatrix} 0 \\ 0 \\ 0 \\ 0 \\ 0 \\ b_{61} \end{bmatrix}$$

$$a_{11} = -\frac{C_a + C_b}{mv_x}, a_{12} = \frac{l_bC_b - l_aC_a}{mv_x} - v_x, a_{15} = \frac{C_a}{m}$$

where $a_{22} = \dfrac{l_bC_b - l_aC_a}{I_zv_x}, a_{23} = -\dfrac{l_a^2C_a + l_b^2C_b}{I_zv_x}, a_{25} = \dfrac{l_aC_a}{I_z},, a_{66} = -\dfrac{B_s}{I_s}$

$$a_{61} = \frac{C_a\eta(t)}{I_sR_s^2v_x}, a_{62} = \frac{C_a\eta(t)l_a}{I_sR_s^2v_x}, a_{65} = -\frac{C_a\eta(t)}{I_sR_s^2}, b_{61} = \frac{1}{I_sR_s}$$

The control output defined as follow:

$$y_p(t) = C_p x_p(t) \tag{7}$$

where $C_p = [0_{5\times1} \quad I_{5\times5}]$.

2.2 IT-2 fuzzy model

Considering the tire cornering stiffness varies along with the road friction, C_a and C_b are redescribed to establish an efficient T-S fuzzy model as [14]:

$$C_a = \sigma_1(t)C_{ao}, C_b = \sigma_1(t)C_{bo} \tag{8}$$

Three prerequisite variables, $\sigma_1(t)$, $\sigma_2(t) = v_x$ and $\sigma_3(t) = \sigma_1(t)/v_x$, are selected to describe the model parameters generated by the time-varying parameters v_x, C_a and C_b. In practice, $\sigma(t)$ is difficult to measure, and due to sensor limitations, longitudinal velocity is difficult to measure accurately, resulting in uncertainty of membership function. Therefore, the IT-2 fuzzy model is used to deal with uncertainty. The three premise variables are represented as:

$$\sigma_i(t) = \theta_{is}(t)\underset{\frown}{\sigma}_i + \theta_{ib}(t)\breve{\sigma}_i \tag{9}$$

where $i = 1,2,3$, the maximum and minimum values of $\sigma_i(t)$ are $\underset{\frown}{\sigma}_i$ and $\breve{\sigma}_i$, the corresponding membership functions are represented by $\theta_{is}(t)$ and $\theta_{ib}(t)$. The membership function is calculated using the following formula:

$$\theta_{is}(t) = \frac{\breve{\sigma}_i - \sigma_i(t)}{\breve{\sigma}_i - \underset{\frown}{\sigma}_i}, \theta_{ib}(t) = \frac{\sigma_i(t) - \underset{\frown}{\sigma}_i}{\breve{\sigma}_i - \underset{\frown}{\sigma}_i} \tag{10}$$

Regarding $\sigma_1(t)$ and $\sigma_2(t)$, the lower and upper membership functions are presented as follows $(i = 1,2)$:

$$\begin{aligned} \theta_{is}^L(t) = \theta_{is}(t)\big|_{+\Delta}, \theta_{is}^U(t) = \theta_{is}(t)\big|_{-\Delta} \\ \theta_{ib}^L(t) = \theta_{ib}(t)\big|_{-\Delta}, \theta_{ib}^U(t) = \theta_{ib}(t)\big|_{+\Delta} \end{aligned} \tag{11}$$

The IT-2 fuzzy model as follows:

Model Rule i: IF $\sigma_1(t)$ is "Small or Big", $\sigma_2(t)$ is "Small or Big" and $\sigma_3(t)$ is "Small or Big", *THEN*

$$\dot{x}_p(t) = A_p x_p(t) + B_{p1}\omega_s(t) + B_{p2}(T_d(t) + T_a(t)) \tag{12}$$

where $i = 1,2,...,8$, A_{p1i}, B_{p1i} and B_{p2i} are obtained by replacing $\sigma_1(t)$, $\sigma_2(t)$ and $\sigma_3(t)$ with corresponding values in matrixes right after (5), respectively. For the $i-th$ model rule, the firing strength is

$$\hat{\phi}(t) = \left[\prod_{i=1}^{3}\theta_i^L(t), \prod_{i=1}^{3}\theta_i^U(t)\right] = [\phi^L(t), \phi^U(t)] \tag{13}$$

The overall IT-2 fuzzy model is shown as:

$$\dot{x}_p(t) = \sum_{i=1}^{8}\phi_i(t)[A_{pi}x_p(t) + B_{p1i}\omega_s(t) + B_{p2i}(T_a(t) + T_d(t))] \tag{14}$$

where $\phi_i = \dfrac{\varsigma_i(t)\phi_i^L(t) + (1-\varsigma_i(t))\phi_i^U(t)}{\sum_{k=1}^{r}\left(\varsigma_k(t)\phi_k^L(t) + (1-\varsigma_k(t))\phi_k^U(t)\right)}$, where $\varsigma_i(t) \in [0,1]$ is a nonlinear function that depends on parametric uncertainty. $\phi_i(t)$ is simplified as ϕ_i and satisfies $0 \le \xi \le 1$.

2.3 Driver steering torque estimation observer

The observer is constructed as follows:

$$\begin{cases} \dot{\hat{x}}_p(t) = \sum_{i=1}^{8}\sum_{j=1}^{8}\zeta_i\zeta_j\{A_{pi}x_p(t) + B_{p2i}[\hat{T}_d(t) + T_a(t)] \\ \qquad + R_j[y_p(t_k h) - \hat{y}_p(t-\tau(t))]\} \\ \dot{\hat{T}}_d(t) = \Gamma\sum_{j=1}^{8}\zeta_j F_j[(y_p(t_k h) - \hat{y}_p(t-\tau(t))) \\ \hat{y}_p(t) = C_p\hat{x}_p(t) \\ e_y(t) = y_p(t_k h) - y_p(k-\tau(t)) \end{cases} \tag{15}$$

By defining the estimated error as: $w(t) = \begin{bmatrix} (x_p(t) - \hat{x}_p(t))^T & (T_d(t) - \hat{T}_d(t))^T \end{bmatrix}^T$, and $g(t) = \begin{bmatrix} \omega_s(t)^T & \dot{\hat{T}}_d^T(t) \end{bmatrix}^T$, the augmented error dynamic system is obtained as:

$$\dot{w}(t) = \sum_{i=1}^{8}\sum_{j=1}^{8}\zeta_i\zeta_j\{A_w w(t) + B_w w(t-\tau(t)) + Gg(t) + F_w e_y(t)\} \tag{16}$$

where $A_w = \begin{bmatrix} A_p & B_{p2} \\ 0 & 0 \end{bmatrix}, B_w = -\tilde{R}_j C_p, G = \begin{bmatrix} B_{p1} & 0 \\ 0 & I \end{bmatrix}, F_w = -\tilde{R}_j, \tilde{R}_j = \begin{bmatrix} R_j \\ F_j \end{bmatrix}$

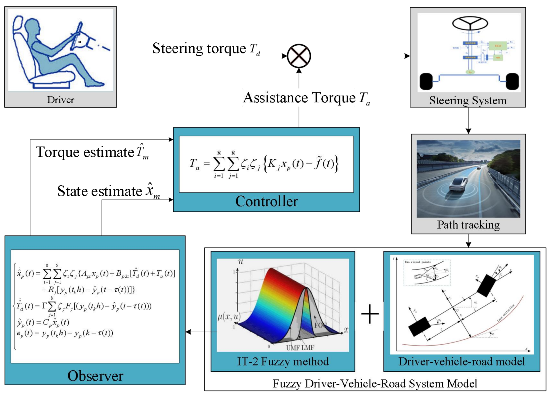

Figure 2. Observer-based fuzzy assistance steering control structure

3 Main result

3.1 Adaptive observer design

In this section, an asymptotically stable IT-2 fuzzy driver steering estimation observer is designed, which satisfies the following constraints:

$$\begin{cases} \|T_d(t) - \hat{T}_d(t)\|_2 \le \gamma_1 \|g(t)\|_2 \\ \|T_d(t) - \hat{T}_d(t)\|_2 \le \gamma_2 \|e_y(t)\|_2 \\ \|x_p(t) - \hat{x}_p(t)\|_2 \le \gamma_3 \|e_y(t)\|_2 \end{cases} \tag{17}$$

Theorem 1: Given positive scalars γ_1, γ_2, ε_m, ε_u, ε_M, if there exist positive matrices P, G_1, G_2, G_3, Q_1, Q_2, Q_3 and general matrices J, Y, H such that

$$\Xi_r < 0 \tag{18}$$

$$\Psi_r < 0 \tag{19}$$

$$\Upsilon_r < 0 \tag{20}$$

$$\begin{bmatrix} G_1 & H \\ * & G_2 \end{bmatrix} > 0 \tag{21}$$

$$\Xi_{ij} = \begin{bmatrix} \Xi_{11} & \Xi_{12} & \Xi_{13} \\ * & \Xi_{22} & \Xi_{23} \\ * & * & \Xi_{33} \end{bmatrix}, \Xi_{11} = \begin{bmatrix} \Xi & P - Y + A_s^T Y^T \\ * & \varepsilon_m^2 G_1 + \varepsilon_u^2 G_2 + \varepsilon_M^2 G_3 - [Y]_s \end{bmatrix}, \Xi_{12} = \begin{bmatrix} Q_1 & \frac{\pi^2}{4} Q_3 - JC \\ * & -JC \end{bmatrix}, \Xi_{13} = \begin{bmatrix} 0 & VL_s \\ 0 & VL_s \end{bmatrix}$$

$$\Xi_{22} = \begin{bmatrix} Q_2 - Q_1 - G_1 - G_2 & G_2 - H \\ * & [H - Q_2]_s - \frac{\pi^2}{4} Q_3 \end{bmatrix}, \Xi_{23} = \begin{bmatrix} H & 0 \\ Q_2 - H & 0 \end{bmatrix}, \Xi_{33} = diag\{-Q - G_2, -\gamma^2 I\}$$

$$\Xi = Q_1 - G_1 - \frac{\pi^2}{4} G_3 + [YA_s]_s + E_1^T E_1, \Psi_{ij} = \begin{bmatrix} \Psi_{11} & \Psi_{12} & \Psi_{13} \\ * & \Psi_{22} & \Psi_{23} \\ * & * & \Psi_{33} \end{bmatrix}, \Psi_{11} = \begin{bmatrix} \Psi & P - Y + A_s^T Y^T \\ * & \varepsilon_m^2 G_1 + \varepsilon_u^2 G_2 + \varepsilon_M^2 G_3 - [Y]_s \end{bmatrix}$$

$$\Psi = Q_1 - G_1 - \frac{\pi^2}{4} G_3 + [YA_s]_s + E_2^T E_2, \Psi_{12} = \Xi_{12}, \Psi_{22} = \Xi_{22}, \Psi_{23} = \Xi_{23}, \Psi_{33} = diag\{-Q_2 - G_2, -\gamma^2 I\},$$

$$E_1 = \begin{bmatrix} 0 & I \end{bmatrix}, E_2 = \begin{bmatrix} I & 0 \end{bmatrix}, \Upsilon_{11} = \Psi_{11}, \Upsilon_{12} = \Psi_{12}, \Upsilon_{13} = \Psi_{13}, \Upsilon_{22} = \Psi_{22}, \Upsilon_{23} = \Psi_{23}$$

Moreover, the observer gain R_j can be derived from $R_j = Y^{-T} J$.

Proof. Consider building a positive Lyapunov function $V(t)$.

$$V(t) = w^T(t)Pw(t) + \int_{t-\varepsilon_m}^{t} w^T(s)Q_1 w(v)ds + \int_{t-\varepsilon_u}^{t-\varepsilon_m} w^T(s)Q_2 w(v)dv$$
$$+ \varepsilon_m \int_{-\varepsilon_m}^{0} \int_{t+\theta}^{t} \dot{w}^T(v)G_1 \dot{w}^T(v)dvd\theta + \varepsilon_M \int_{-\varepsilon_u}^{-\varepsilon_m} \int_{t+\theta}^{t} \dot{w}^T(v)G_2 \dot{w}(v)dvd\theta$$
$$- \frac{\pi^2}{4} \int_{nh}^{t} [w(v) - w(nh)]^T G_3 [w(v) - w(nh)]dv + \varepsilon_u^2 \int_{nh}^{t} \dot{w}^T(v)G_3 \dot{w}(v)dv$$

Time derivative of $V(t)$ is obtained as

$$\dot{V}(t) = 2w^T(t)P\dot{w}(t) + w^T(t)Q_1 w(t) - w^T(t-\varepsilon_u)Q_2 w(t-\varepsilon_u) + w^T(t-\varepsilon_m)(Q_2 - Q_1)w(t-\varepsilon_m)$$
$$- \varepsilon_m \int_{t-\varepsilon_m}^{t} \dot{w}^T(v)G_1 \dot{w}(v)dv - \varepsilon_M \int_{t-\varepsilon_u}^{t-\varepsilon_m} \dot{w}^T(v)G_2 \dot{w}(v)dv + \varepsilon_m^2 \dot{w}^T(v)G_1 \dot{w}(v) + \varepsilon_M^2 \dot{w}^T(v)G_2 \dot{w}(v) \tag{22}$$
$$+ d_u^2 \dot{w}^T(v)G_3 \dot{w}(v) - \frac{\pi^2}{4}[w(t) - w(t-d(t))]^T G_3 [w(t) - w(t-d(t))]$$

For the general matrix Y we can get the following equation:

$$[w^T(t)Y + \dot{w}^T(t)\lambda Y][A_w w(t) + B_w w(t-\tau(t)) + Gg(t) + F_w e_y(t) - \dot{w}(t)] = 0 \tag{23}$$

By combining the above formula, by defining $J = Y^T \tilde{L}$ and $e_y(t) = 0$, we can get:

$$\dot{V}(t) + [T_d(t) - \hat{T}_d(t)]^T [T_d(t) - \hat{T}_d(t)] - \gamma_1^2 g^T(t)g(t) \le \sum_{i=1}^{q} \sum_{j=1}^{q} \zeta_i \zeta_j \varphi_1^T(t) \Xi_r \varphi_1(t) \tag{24}$$

where $\varphi_1^T(t) = col\{w(t), \dot{w}(t), w(t-d_m), w(t-d(t)), w(t-d_u), \omega_s(t)\}$. Under zero initial conditions and $\Xi_r < 0$ in (18), it can effectively guarantee the performance of $\left\| T_d(t) - \hat{T}_d(t) \right\|_2 \le \gamma_1 \left\| e_y(t) \right\|_2$ in (17).

Secondly, consider $g(t) = 0$ in the constraint (17), the following function $J_2(t)$ satisfies

$$\dot{V}(t) + [T_d(t) - \hat{T}_d(t)]^T [T_d(t) - \hat{T}_d(t)] - \gamma_2^2 \omega_s^T(t) \omega_s(t) \le \sum_{i=1}^{q} \sum_{j=1}^{q} \zeta_i \zeta_j \varphi_2^T(t) \Psi_r \varphi_2(t) \tag{25}$$

where $\varphi_2^T(t) = col\{w(t), \dot{w}(t), w(t-d_m), w(t-d(t)), w(t-d_u), e_y(t)\}$. Under $\Psi_r < 0$ in (19), it allows the constraint $\left\| T_d(t) - \hat{T}_d(t) \right\|_2 \le \gamma_2 \left\| g(t) \right\|_2$ in (17) can be guaranteed.

Similarly, when $g(t) = 0$, the following condition is true as:

$$\dot{V}(t)+[x_p(t)-\hat{x}_p(t)]^T[x_p(t)-\hat{x}_p(t)]-\gamma_3^2\omega_s^T(t)\omega_s(t)\leq\sum_{i=1}^{q}\sum_{j=1}^{q}\zeta_i\zeta_j\varphi_3^T(t)\Upsilon_r\varphi_3(t) \tag{26}$$

Therefore, the above proof can ensure that the error dynamics in (16) is stable and the constrains in (17) are guarantee. Proof complete.

3.2 Adaptive controller design

Substituting (4) into (6), the driver–vehicle model is obtained as [15]:

$$\dot{x}_p(t)=\overline{A}_p x_p(t)+B_{p1}\omega_s(t)+B_{p2}(T_a(t)+\tilde{f}(t)) \tag{27}$$

where

$$\overline{A}_p=\begin{bmatrix} a_{11} & a_{12} & 0 & 0 & a_{15} & 0\\ a_{22} & a_{23} & 0 & 0 & a_{25} & 0\\ 1 & l_d & 0 & v_x & 0 & 0\\ 0 & 1 & 0 & 0 & 0 & 0\\ 0 & 0 & 0 & 0 & 0 & -1\\ \hat{a}_{61} & \hat{a}_{62} & \lambda k_{s1} & \lambda T_{s3} & \hat{a}_{65} & a_{66} \end{bmatrix}$$

$$\hat{a}_{61}=a_{61}+\lambda T_{s1},\hat{a}_{62}=a_{62}+\lambda T_{s2},\hat{a}_{65}=a_{65}+\lambda T_{s4},\hat{T}_d(t)-T_d(t)=\tilde{f}(t)$$

By estimating the steering torque of the driver, an adaptive controller can be designed. Firstly, the proposed controller is as follows:

$$T_a=\sum_{i=1}^{8}\sum_{j=1}^{8}\zeta_i\zeta_j\left\{K_j x_p(t)-\tilde{f}(t)\right\} \tag{28}$$

where the local control gain K_i needs to be designed.

Therefore, combining equations (26) and (27), the IT-2 fuzzy model of the closed-loop system can be described as:

$$\dot{x}_p(t)=\sum_{i=1}^{8}\sum_{j=1}^{8}\zeta_i\zeta_j\{(\overline{A}_p+B_{p2}K_j)x_p(t)+B_{p1}\omega_s(t)\} \tag{29}$$

In brief, the adaptive steering controller is proposed to make the system (26) be stable and satisfy the following performance as:

$$\left\|y_p(t)\right\|_2<\gamma\left\|\omega_s(t)\right\|_2 \tag{30}$$

Theorem 2: Given positive scalars $\gamma^3,\alpha_1,\alpha_2$, if there exist positive matrices $\overline{W}_1,\overline{W}_2,\overline{W}_3,\overline{N}_1,\overline{N}_2$ and general matrices $\overline{U},\overline{G}$ such that $(i,j=1,2,...,8)$

$$\overline{\Phi}_{ii}<0 \tag{31}$$

$$\overline{\Phi}_{ij}+\overline{\Phi}_{ji}<0, i<j \tag{32}$$

$$\overline{\Phi}_{ij}=\begin{bmatrix} \overline{\Theta}_{ij}^{11} & \overline{\Theta}_{ij}^{12} & \overline{\Theta}_{ij}^{13}\\ * & \overline{\Theta}_{22} & 0\\ * & * & \overline{\Theta}_{33} \end{bmatrix} \tag{33}$$

where

$$\overline{\Theta}_{ij}^{11}=\begin{bmatrix} \overline{\Theta} & \overline{W}_1 & \frac{\pi^2}{4}\overline{W}_3 & 0 & B_{1i}\\ * & \overline{N}_2-\overline{N}_1-\overline{W}_1-\overline{W}_2 & \overline{W}_2-\overline{U} & \overline{U} & 0\\ * & * & [\overline{U}-\overline{W}_2]_s-\frac{\pi^2}{4}\overline{W}_3 & \overline{W}_2-\overline{U} & 0\\ * & * & * & -\overline{N}_2-\overline{W}_2 & 0\\ * & * & * & * & -\gamma^2 I \end{bmatrix},\overline{\Theta}_{ij}^{12}=\begin{bmatrix} \alpha_1\overline{R}\overline{A}_{pi}^T & (\alpha_2-\alpha_1)\overline{R}\overline{A}_{pi}^T & \alpha_2\overline{R}\overline{A}_{pi}^T\\ 0 & 0 & 0\\ 0 & 0 & 0\\ 0 & 0 & 0\\ \alpha_1 B_{1i}^T & (\alpha_2-\alpha_1)B_{1i}^T & \alpha_2 B_{1i}^T \end{bmatrix},\overline{\Theta}_{ij}^{13}=\begin{bmatrix} C_{pi}^T\\ 0\\ 0\\ 0\\ 0 \end{bmatrix}$$

$$\overline{\Theta}=[\overline{R}(\overline{A}_{pi}+B_{2i}\overline{K}_j)]_s+\overline{N}_1-\overline{W}_1-\frac{\pi^2}{4}\overline{W}_3+C^TC,\overline{\Theta}_{22}=diag\{-\overline{W}_1^{-1},-\overline{W}_2^{-1},-\overline{W}_3^{-1}\},\overline{\Theta}_{33}=-I$$

Then, the system in (28) satisfies the asymptotic stability and the constrain $\|y_p(t)\|_2<\gamma\|\omega_s(t)\|_2$. Moreover, the feedback gain K_j of the controller can be estimated as $K_j=\overline{K}_j\overline{R}^{-1}$.

4 Performance simulation result

In this part, the effectiveness of the proposed assistance control method is proved by simulation. Table 2 gives the model parameters used in the simulation.

Fig. 3 (a) provides the variation result of road curvature in a lane change maneuver. Fig. 3 (b) and Fig. 3 (c) depicts the simulation results of the driver's steering torque and assistance torque. It can be seen from Fig. 3 (b) that the steering torque with control is less than without control. Therefore, the proposed control method can reduce the driver's torque and thus improve the driving comfort.

Fig. 4 shows the path tracking performances such as (a) lateral velocity, (b) heading error, (c) lateral offset, (d) yaw rate, (e) front wheel steering rate, and (f) front wheel steering angle. As can be seen from Fig. 4(a) and (b), the proposed control method can effectively reduce the lateral offset and lateral velocity, and improve the path tracking effect. From the Fig. 4(b) and (d), the adaptive controller can reduce the yaw rate and heading error, and make their changes smoother, indicating that the controller has good stability. Fig. 4(e) and (f) shows front wheel steering rate and front wheel steering angle, respectively. This indicates that the front wheel steering angle falls within the acceptable range.

The global trajectory of the vehicle is shown in Figure 5, which shows that the driver can use adaptive control methods to achieve the desired path. However, the proposed adaptive control method produces less fluctuation than the uncontrolled method. This also verifies the superiority of the adaptive control method proposed in this paper in improving the performance of path tracking.

Table 1. Model parameters

Symbol	value	Symbol	value
m	1370 kg	I_s	2315 kg·m^2
l_m	1.4 m	l_n	1.5 m
C_m	67208 N/rad	C_n	66218 N/rad
l_d	5 m	I_s	0.05 kg·m^2
B_s	5.73 Nm/rad/s	R_s	22
η_t	0.185 m	T_l	3 s
T_i	0.3 s	T_n	0.1 s
K_c	10	K_a	30

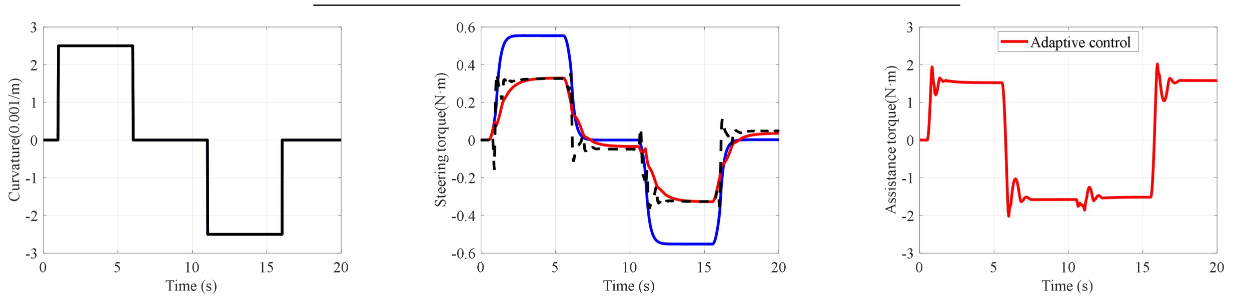

(a) Road curvature **(b) Steering torque** **(c) Assistance torque**

Figure 3. Simulation inputs for road curvature and simulation results

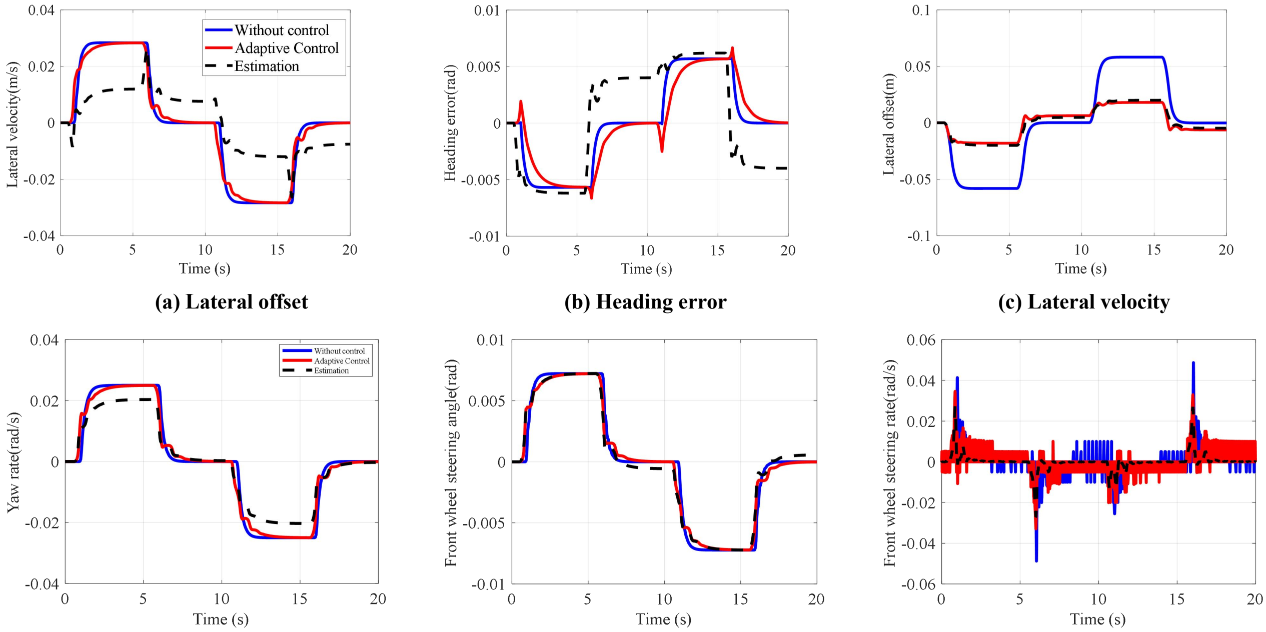

(a) Lateral offset **(b) Heading error** **(c) Lateral velocity**

(d) Yaw rate **(e) Front wheel steering angle** **(f) Front wheel steering rate**

Figure 4. Simulation results

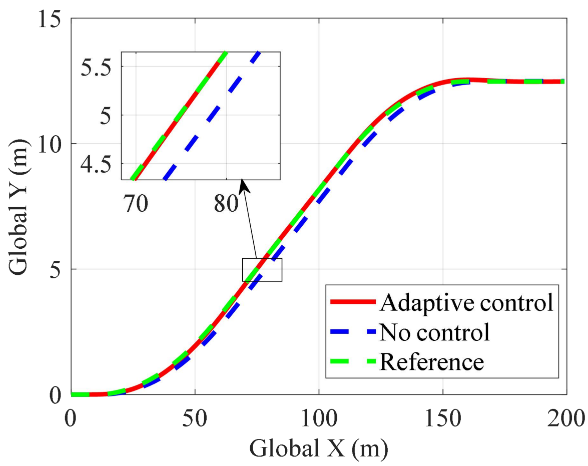

Figure 5. Simulation result for global trajectories

5 Conclusion

This paper presented an observe-based driver adaptive assistance control method for path tracking system. Firstly, considering the driver's steering behavior, vehicle kinematics and lateral dynamics, an interval Type-2 fuzzy model was established to describe the global driver-vehicle-road system model, which can effectively deal with the system uncertainty caused by the time-varying characteristics of longitudinal velocity. Secondly in order to obtain the driver's steering torque information, an adaptive observer was designed to effectively estimate the driver's steering torque. The obtained observer has a great contribution to improving the accuracy of the system state and driver's steering torque estimation. Then, by solving linear matrix inequalities, an adaptive steering control method was proposed to reduce the driver's burden and improve the performance of vehicle path tracking. Finally, the effectiveness of the proposed control method was verified by simulation.

Acknowledgement

This work is supported by the National Natural Science Foundation of China (Grant No. 52302469), the Guangdong Basic and Applied Basic Research Foundation (Grant Nos. 2022A1515011495, 2022A1515110301, 2023A1515012327 and 2024A1515010449), the research grant of the University of Macau (Grant Nos. MYRG 2022-00099-FST, MYRG GRG2023-00235-FST-UMDF and MYRG-CRG 2022-00006-FST), the Zhuhai Science and Technology Innovation Bureau (Grant No. 2220004003107), and Yunfu Science and Technology Project (Grant No. S2023090104).

References

[1] Y. Liu, Q. Xu, H. Guo. A type-2 fuzzy approach to driver-automation shared driving lane keeping control of semi-autonomous vehicles under imprecise premise variable. Chinese Journal of Mechanical Engineering, 2022, 35(1):1-18.

[2] Marcano M, Díaz S, Pérez J, et al. A review of shared control for automated vehicles: theory and applications, IEEE Transactions on Human-Machine Systems, 2020, 50(6): 475-491.

[3] J. Liang et al. Robust shared control system for aggressive driving based on cooperative modes identification. IEEE Transactions on Systems, 2023, 53(11): 6672-6684.

[4] Chu S, Xie Z, Wong P K, et al. Observer-based gain scheduling path following control for autonomous electric vehicles subject to time delay. Vehicle System Dynamics, 2021, 60(5): 1602-1626.

[5] Cao H, Fink O, Gu E F, et al. Path tracking control for autonomous vehicles using hybrid fault-tolerant approach. Proceedings of the Institution of Mechanical Engineers, Part C: Journal of Mechanical Engineering Science, 2024, 238(13):6738-6747.

[6] C. Hu, Y. Chen and J. Wang. Fuzzy observer-based transitional path-tracking control for autonomous vehicles. IEEE Transactions on Intelligent Transportation Systems, 2021, 22(5): 3078-3088.

[7] W. Li, X. Wang, J. Zhao, C. Gao and Z. Xie. Fuzzy output feedback steering control of lane keeping assistance systems with aperiodic sampling. IEEE/ASME Transactions on Mechatronics, 2024, 29(3): 1726-1737.

[8] F. Ding, H. Shan, X. Han, C. Jiang, C. Peng, and J. Liu. Security-based resilient triggered output feedback lane keeping control for human–machine cooperative steering intelligent heavy truck under denialof-service attacks. IEEE Transactions on Fuzzy Systems, 2023, 31(7): 2264-2276.

[9] A.-T. Nguyen, C. Sentouh and J.-C. Popieul. Driver-automation cooperative approach for shared steering control under multiple system constraints: design and experiments. IEEE Transactions on Industrial Electronics, 2017, 64(5): 3819-3830.

[10] X. Wang, L. Guo and Y. Jia. Online sensing of human steering intervention torque for autonomous driving actuation systems. IEEE Sensors Journal, 2018, 18(8): 3444-3453.

[11] A. Marouf, M. Djemaï, C. Sentouh and P. Pudlo. Driver torque and road reaction force estimation of an electric power assisted steering using sliding mode observer with unknown inputs. International IEEE Conference on Intelligent Transportation Systems, 2010, doi: 10.1109/ITSC.2010.5625043.

[12] A.-T. Nguyen, T.-M. Guerra, C. Sentouh and J.-C. Popieul. Decoupling-based LPV observer for driver torque intervention estimation in human–machine shared driving under uncertain vehicle dynamics. IEEE Transactions on Automation Science and Engineering, 2024, doi: 10.1109/TASE.2024.3394240.

[13] Rodrigues M, Hamdi H, Theilliol D, et al. Actuator fault estimation based adaptive polytopic observer for a class of LPV descriptor systems. John Wiley & Sons, Ltd, 2015, 25(5): 673-688.

[14] Liu Y, Xu Q, Guo H, et al. A type-2 fuzzy approach to driver-automation shared driving lane keeping control of semi-autonomous vehicles under imprecise premise variable, Chinese Journal of Mechanical Engineering, 2022, 35(1):1-18.

[15] Zhou S, Ju Z, Liu Y, et al. Driver state detection for driver-automation shared control with fuzzy logic. Control Engineering Practice, 2022, DOI:10.1016/j. conengprac.2022.105